

Atomic data from the IRON Project

L. Electron impact excitation of Fe XIX*

K. Butler¹ and C. J. Zeippen²

¹ Institut für Astronomie und Astrophysik, Scheinerstr. 1, 81679 München, Germany

² UMR 8631 (associée au CNRS et à l'Université Paris 7) et DAEC, Observatoire de Paris, 92195 Meudon, France

Received 2 February 2001 / Accepted 11 April 2001

Abstract. Collision strengths and collisional rate parameters have been calculated for transitions among 92 $n = 2$ and $n = 3$ levels of O-like Fe XIX. The method used is the Breit-Pauli R-matrix formalism in which most prominent relativistic effects are accounted for. Partial wave contributions up to $J = 59/2$ are included explicitly while “top-up” procedures complete the sum to infinity. Several thousand energy points were used to fully incorporate the effect of resonances in the collisional cross sections when estimating the collisional rate parameters. This is particularly important at lower temperatures where the resonant contributions dominate. The present results are expected to be accurate to better than 20% for transitions among $n = 2$ levels.

Key words. atomic and molecular data

1. Introduction

This is the third and final paper in a short series devoted to CNO-like iron. The work has been carried out under the auspices of the Iron Project (IP), an international collaboration formed to provide atomic data of astrophysical interest, particularly for iron group elements. The overall methods and aims have been chronicled in detail in Hummer et al. (1993), the first paper in the IP series. At present, fifty publications have been presented giving results for collisional and radiative data for a wide variety of systems. The home page for the project with a full list of papers is presently to be found at

<http://www.usm.uni-muenchen.de/...>
[... people/ip/iron-project.html](http://www.usm.uni-muenchen.de/people/ip/iron-project.html).

The launch of the SOHO satellite in 1995 was the main motivating influence which initiated the creation of the IP and observations of Fe XIX in the sun have been made with the CDS instrument by Czaykowska et al. (1999). However, these authors only report velocity measurements. On the other hand, Schrijver et al. (1995) have used the Extreme Ultraviolet Explorer (EUVE, Bowyer & Malina 1991) to obtain spectra of the corona of seven cool stars. They analyzed these spectra using the calculations

Send offprint requests to: K. Butler,
e-mail: butler@usm.uni-muenchen.de

* Detailed tables of the present data are available in electronic form at the CDS via anonymous ftp to [cdsarc.u-strasbg.fr](ftp://cdsarc.u-strasbg.fr) (ftp 130.79.128.5) or via <http://cdsweb.u-strasbg.fr/cgi-bin/qcat?J/A+1/372/1083>

of Mewe et al. (1985, 1986) to derive the densities and temperatures of these objects. Interest in the X-ray region has been further enhanced with the launch of the Chandra and XMM satellites. These provide high resolution observations increasing the need for accurate atomic data for their analysis.

Fe XIX has been the subject of several previous calculations, all of them in the distorted wave approximation. The earlier work therefore does not include the resonance contributions which, as we shall see, have a major impact on the collision rates. The first reported calculation for O-like iron was that of Louergue et al. (1985) who not only provided estimates of the collisional data but also tabulated radiative data for this ion. They confined themselves to a treatment of the $n = 2$ complex, however. Following on from this, Bhatia et al. (1989) also provided distorted wave data, this time including the $2s^2 2p^3 3s$ and $2s^2 2p^3 3d$ configurations. Both these calculations included relativistic effects by performing an algebraic transformation on the LS-coupling data using JAJOM (Saraph 1972). Very recently, Zhang and Sampson (priv. commun.) have computed collisional data in a relativistic distorted wave approximation, thus including the relativistic effects explicitly but still omitting the resonance contribution.

Given the increasing interest in the iron ions from the observational side on the one hand, and the power of the new theoretical methods described by Hummer et al. (1993) on the other, it is natural to attempt to provide more accurate and extensive data to be used in the observational analysis. That is the purpose of the present paper. In Sect. 2 we present such details of the method

Table 1. The λ parameters for Fe XIX.

$n\ell$	$\lambda_{n\ell}$	$n\ell$	$\lambda_{n\ell}$
1s	1.40693	3s	1.19318
2s	1.27800	3p	1.15098
2p	1.20603	3d	1.21411

as are necessary to outline the calculation, in particular, the target is described and the energies and oscillator strengths derived from the target wavefunctions are compared with data from other sources. These are generally indicators of the accuracy of the target wavefunctions and thus of the calculation as a whole. The results are then summarized in Sect. 3 and a comparison is made with previous work. We close the section and the paper with an outlook on future prospects.

2. Method

The methods are the same as have been used throughout the IP series and the interested reader is referred to Hummer et al. (1993) for full details. Here we concentrate on the specifics with regard to O-like iron.

The calculation is similar in scope to those on C-like (Butler & Zeippen 2000) and N-like iron (Butler & Zeippen 2001) we have reported previously. The target wavefunctions were obtained using a version of the SUPERSTRUCTURE program (Eissner et al. 1974) due to Nussbaumer & Storey (1978) and comprises 12 configurations, namely

$$\begin{aligned}
 &2s^2 2p^4 \quad 2s2p^5 \quad 2p^6 \\
 &2s^4 2p^3 3s \quad 2s^4 2p^3 p \quad 2s^4 2p^3 d \\
 &2s2p^4 3s \quad 2s2p^4 3p \quad 2s2p^4 3d \\
 &2p^5 3s \quad 2p^5 3p \quad 2p^5 3d
 \end{aligned}$$

the first six of which were included explicitly in the target, while the latter six only provided correlation. This gives a 46 term target in LS-coupling which in turn leads to a 92 level Breit-Pauli approximation. Note that a few intervening levels belonging to the $2s2p^4 3s$ configuration are also included as they lie within the energy region under consideration. The target energies were obtained by minimizing the sum of the energies of all the terms in all the configurations by adjusting the free parameters occurring in the Thomas-Fermi-Dirac-Amaldi potential used to describe the one-electron orbitals. The resulting $\lambda_{n\ell}$ which depend on both n and ℓ are to be found in Table 1. While this procedure is not optimal for the 46 terms which are the subject of the present investigation it will facilitate comparison with more ambitious calculations including the $n = 4$ levels at a later date. In any case, the resulting wavefunctions do describe the levels accurately as is evidenced by the good agreement between the calculated energies and observed values of Corliss & Sugar (1982) shown in Table 2. The accuracy is of order 1% although only relatively few levels have been observed. Again we can compare the oscillator strengths derived from these

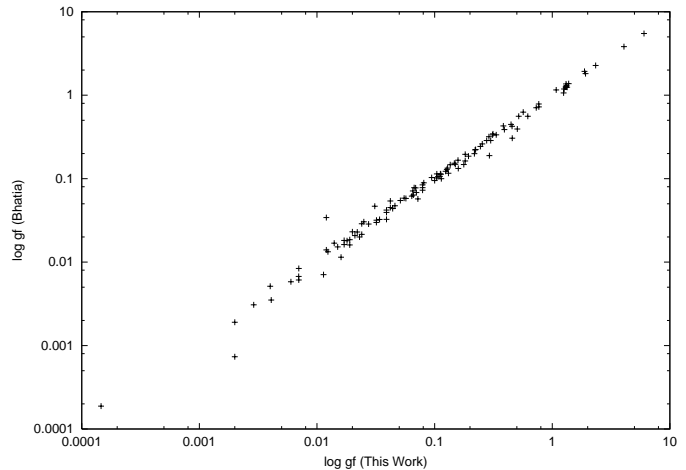


Fig. 1. Comparison of the gf -values obtained in the present Fe XIX target calculation with those of Bhatia et al. (1989) and Louergue et al. (1985).

wavefunctions with those of Louergue et al. (1985) for the $n = 2$ transitions and those of Bhatia et al. (1989) for transitions into the $n = 3$ levels. This has been done in Fig. 1 where the agreement is seen to be excellent. Thus we can be confident that the wavefunctions provide a good description of the Fe^{18+} target. The complete set of oscillator strengths is available in electronic form and may be used to obtain the high energy limits of the allowed transitions as described by Burgess & Tully (1992).

These wavefunctions were then used as the basis for the electron scattering calculation which was performed with an unpublished R-matrix package due to Eissner based on the programs described by Berrington et al. (1995). One body relativistic effects are included in a Breit-Pauli approximation. Contributions to the total angular momentum up to $J = 59/2$ were included explicitly, the remaining sum to infinity being “topped-up” either by the use of the Coulomb-Bethe approximation as implemented by Eissner et al. (1999) for intermediate coupling for the allowed transitions or, for the forbidden transitions, by a geometric progression. Such procedures were previously described by Burke & Seaton (1986) for the LS-coupling case. The importance of these contributions has been discussed more fully in an earlier paper (Butler & Zeippen 2000). We simply note here that they are significant only at the highest energies.

A grid of collision strengths was obtained by matching the inner region R-matrices which are energy independent to Coulomb functions in the outer region for several thousand energy points. These data were convolved with a Maxwellian distribution and the resulting effective collision strengths are tabulated in Table 3 which is available electronically at the CDS. Here a grid of temperatures covering the maximum ionic abundance as given by Arnaud and Rothenflug (1985) is provided. At the very highest temperatures there is a contribution from energies beyond the range of our energy grid. Here we have simply extrapolated the last calculated point to the higher energies. Since

Table 2. Calculated versus observed (Sugar & Corliss 1985) target energies (cm^{-1}).

Index	Term	E_{calc}	E_{obs}	Index	Term	E_{calc}	E_{obs}
1	$2s^2 2p^4$	${}^3P_2^e$	0.	47	$2s^2 2p^3 3p$	${}^3P_0^e$	7228384.
2	$2s^2 2p^4$	${}^3P_0^e$	74766.	48	$2s^2 2p^3 3p$	${}^3P_1^e$	7230047.
3	$2s^2 2p^4$	${}^3P_1^e$	90160.	49	$2s^2 2p^3 3p$	${}^3D_3^e$	7230553.
4	$2s^2 2p^4$	${}^1D_2^e$	174400.	50	$2s^2 2p^3 3d$	${}^3D_2^e$	7239231.
5	$2s^2 2p^4$	${}^1S_0^e$	328726.	51	$2s^2 2p^3 3p$	${}^1P_1^e$	7256101.
6	$2s^2 2p^5$	${}^3P_2^e$	932013.	52	$2s^2 2p^3 3p$	${}^3P_2^e$	7261458.
7	$2s^2 2p^5$	${}^3P_1^e$	995686.	53	$2s^2 2p^3 3d$	${}^3D_1^e$	7264817.
8	$2s^2 2p^5$	${}^3P_0^e$	1041743.	54	$2s^2 2p^3 3d$	${}^3D_3^e$	7266108. 7249000
9	$2s^2 2p^5$	${}^1P_1^e$	1287358.	55	$2s^2 2p^3 3p$	${}^1D_2^e$	7290783.
10	$2p^6$	${}^1S_0^e$	2168921.	56	$2s^2 2p^3 3d$	${}^3F_2^e$	7331492.
11	$2s^2 2p^3 3s$	${}^5S_2^o$	6643177.	57	$2s^2 2p^3 3d$	${}^3F_3^e$	7344715.
12	$2s^2 2p^3 3s$	${}^3S_1^o$	6695619.	58	$2s^2 2p^3 3d$	${}^1S_0^o$	7344886.
13	$2s^2 2p^3 3s$	${}^3D_2^o$	6799977.	59	$2s^2 2p^3 3d$	${}^3G_3^o$	7349984.
14	$2s^2 2p^3 3s$	${}^3D_1^o$	6801973.	60	$2s^2 2p^3 3d$	${}^3G_4^o$	7352018.
15	$2s^2 2p^3 3s$	${}^3D_3^o$	6835715.	61	$2s^2 2p^3 3d$	${}^1P_1^o$	7353361.
16	$2s^2 2p^3 3s$	${}^1D_2^o$	6855497.	62	$2s^2 2p^3 3d$	${}^3F_4^o$	7376385.
17	$2s^2 2p^3 3p$	${}^5P_1^e$	6877623.	63	$2s^2 2p^3 3d$	${}^1G_4^o$	7389397.
18	$2s^2 2p^3 3p$	${}^5P_2^e$	6881746.	64	$2s^2 2p^3 3d$	${}^3G_5^o$	7389701.
19	$2s^2 2p^3 3p$	${}^5P_3^e$	6900633.	65	$2s^2 2p^3 3p$	${}^1S_0^e$	7391370.
20	$2s^2 2p^3 3s$	${}^3P_0^o$	6913096.	66	$2s^2 2p^3 3d$	${}^3P_2^o$	7394243. 7370000
21	$2s^2 2p^3 3s$	${}^3P_1^o$	6921107.	67	$2s^2 2p^3 3d$	${}^3P_1^o$	7402113.
22	$2s^2 2p^3 3p$	${}^3P_1^e$	6932129.	68	$2s 2p^4 3s$	${}^5P_3^o$	7412538.
23	$2s^2 2p^3 3p$	${}^3P_2^e$	6953781.	69	$2s^2 2p^3 3d$	${}^3D_3^o$	7417913. 7396000
24	$2s^2 2p^3 3p$	${}^3P_0^e$	6962365.	70	$2s^2 2p^3 3d$	${}^3P_0^o$	7418927.
25	$2s^2 2p^3 3s$	${}^3P_2^o$	6978533.	71	$2s^2 2p^3 3d$	${}^3D_2^o$	7423125. 7405000
26	$2s^2 2p^3 3s$	${}^1P_1^o$	6994093.	72	$2s^2 2p^3 3d$	${}^3P_1^o$	7424093.
27	$2s^2 2p^3 3p$	${}^3D_1^e$	7010957.	73	$2s^2 2p^3 3d$	${}^1D_2^o$	7432691.
28	$2s^2 2p^3 3p$	${}^3F_2^e$	7033918.	74	$2s^2 2p^3 3d$	${}^3S_1^o$	7445530.
29	$2s^2 2p^3 3p$	${}^3D_2^e$	7051211.	75	$2s 2p^4 3s$	${}^5P_2^e$	7460913.
30	$2s^2 2p^3 3p$	${}^3F_3^e$	7055314.	76	$2s^2 2p^3 3d$	${}^1F_3^o$	7469769. 7449000
31	$2s^2 2p^3 3p$	${}^1P_1^e$	7067538.	77	$2s^2 2p^3 3d$	${}^3F_2^o$	7476405.
32	$2s^2 2p^3 3p$	${}^3D_3^e$	7070019.	78	$2s^2 2p^3 3d$	${}^3F_3^o$	7483374. 7450000
33	$2s^2 2p^3 3p$	${}^1F_3^e$	7090868.	79	$2s 2p^4 3s$	${}^5P_1^e$	7494218.
34	$2s^2 2p^3 3p$	${}^3F_4^e$	7095566.	80	$2s^2 2p^3 3d$	${}^3D_2^o$	7500485. 7554000
35	$2s^2 2p^3 3p$	${}^3P_0^e$	7110865.	81	$2s 2p^4 3s$	${}^3P_2^e$	7515042.
36	$2s^2 2p^3 3p$	${}^3P_1^e$	7132460.	82	$2s^2 2p^3 3d$	${}^3D_1^o$	7517804.
37	$2s^2 2p^3 3p$	${}^3P_2^e$	7150900.	83	$2s^2 2p^3 3d$	${}^3F_4^o$	7522089.
38	$2s^2 2p^3 3p$	${}^3D_1^e$	7154659.	84	$2s^2 2p^3 3d$	${}^3P_0^o$	7525441.
39	$2s^2 2p^3 3p$	${}^1D_2^e$	7179196.	85	$2s^2 2p^3 3d$	${}^3P_2^o$	7537621.
40	$2s^2 2p^3 3p$	${}^3S_1^e$	7183366.	86	$2s^2 2p^3 3d$	${}^3D_1^o$	7543025. 7567000
41	$2s^2 2p^3 3p$	${}^3D_2^e$	7184580.	87	$2s^2 2p^3 3d$	${}^3D_3^o$	7559454.
42	$2s^2 2p^3 3d$	${}^5D_0^o$	7188083.	88	$2s 2p^4 3s$	${}^3P_1^e$	7566119.
43	$2s^2 2p^3 3d$	${}^5D_2^o$	7188830.	89	$2s^2 2p^3 3d$	${}^1F_3^o$	7583729. 7565000
44	$2s^2 2p^3 3d$	${}^5D_1^o$	7188874.	90	$2s^2 2p^3 3d$	${}^1D_2^o$	7584033.
45	$2s^2 2p^3 3d$	${}^5D_3^o$	7189349.	91	$2s^2 2p^3 3d$	${}^3P_0^e$	7585803.
46	$2s^2 2p^3 3d$	${}^5D_4^o$	7193725.	92	$2s^2 2p^3 3d$	${}^1P_1^o$	7644484. 7606000

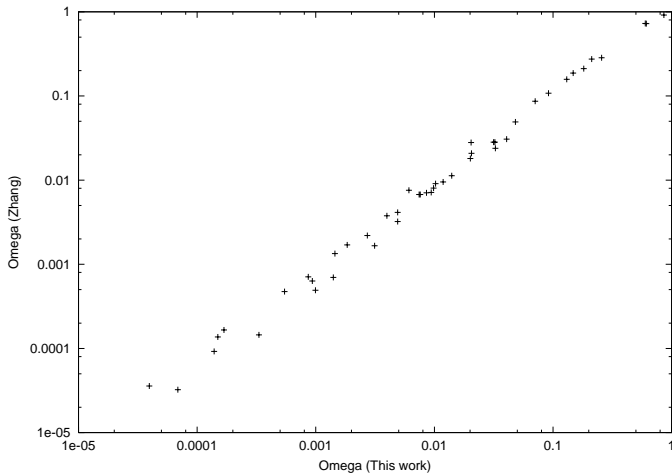


Fig. 2. Comparison of the collision strengths obtained in the present calculation with those of Zhang & Sampson (2001).

the contribution is still relatively small the overall error caused by the use of this procedure is not significant within the estimated errors for the calculation as a whole.

3. Results and discussion

Collision strengths are provided for all transitions amongst the 92 target terms, whereby it is clear that data involving the $n = 3$ levels will be of lower accuracy than those for the $n = 2$ transitions, which may be expected to be accurate to better than 20%. For the higher energies, above the last target term at 70 Ryd, we can compare our results with the relativistic distorted wave collision strengths of Zhang & Sampson (2001) which is done in Fig. 2. The figure demonstrates the good agreement between the two completely independent methods and confirms the accuracy of *both* calculations. The same can be done for the data of Louergue et al. (1985) and Bhatia et al. (1989) for the $n = 2$ and $n = 3$ transitions respectively (Fig. 3). Although the scatter is larger due to the larger uncertainties in the $n = 3$ transitions, the agreement is still satisfactory.

However, all the distorted wave calculations omit the resonance contributions. That these can play a significant rôle is graphically demonstrated in Fig. 4 which shows the energy dependence of the $2s^22p^4\ ^3P_2^e - 2s^22p^4\ ^3P_0^e$ transition in Fe XIX. The distorted wave results give only the background and thus underestimate the cross section. The resonance contribution becomes increasingly important at lower temperatures since the Maxwellian distribution then gives more weight to the lower energy region. Thus our rates will be a major improvement on the distorted wave values in photoionized plasmas for example. On the other hand, the accuracy of the calculated positions of the resonances becomes increasingly relevant as the temperature is decreased. This accuracy is affected by a number of factors but a major component is the lack of experimentally determined target energy levels. An error of only a few per cent in the calculated target energies translates

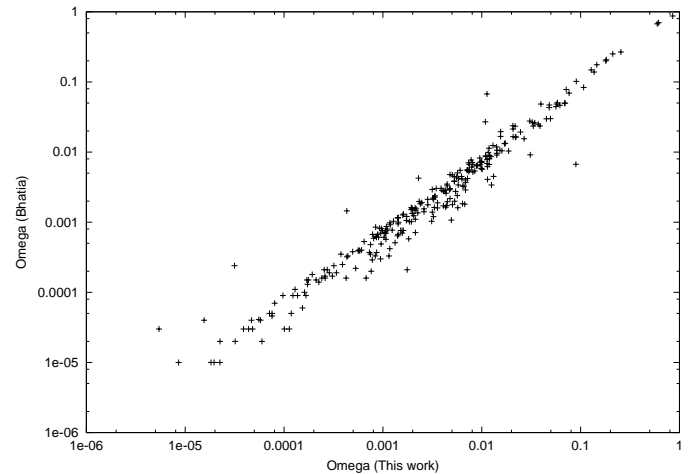


Fig. 3. Comparison of the collision strengths obtained in the present calculation with those of Bhatia et al. (1989) and Louergue et al. (1985).

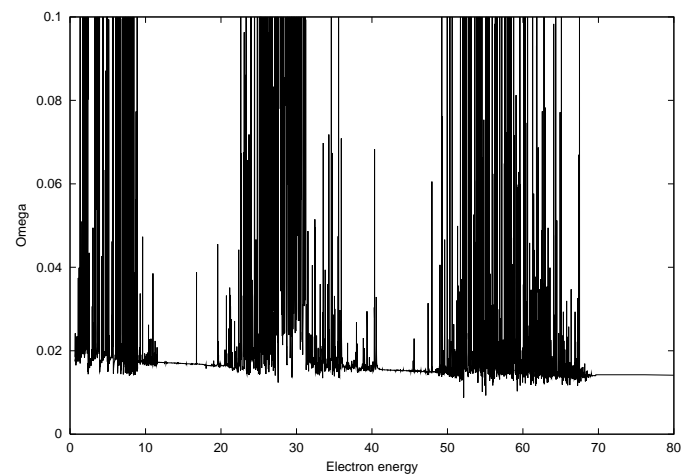


Fig. 4. Omega for the $2s^22p^4\ ^3P_2^e - 2s^22p^4\ ^3P_0^e$ transition of Fe XIX.

directly to a similar error in the resonant positions. Resonances close to threshold are especially important and small shifts in their positions have a large impact on the calculated rates. For this reason we tabulate the effective collision strengths only down to a temperature of $\log T = 5.0$.

Our own results for the $n = 3$ transitions omit resonances converging to the $n = 4$ levels and beyond and are thus significantly less accurate than the data for the lower levels. This has been demonstrated by the very recent extensive calculations for C-like iron performed by Badnell & Griffin (2001). They used a frame transformation technique to obtain data including the $n = 4$ states and found large differences from our own earlier calculations (Butler & Zeippen 2000) for this ion.

Thus, in summary, we can be confident that our data for the $n = 2$ transitions are accurate to perhaps 20%. At the same time we intend to carry out improved calculations for this and other ions of the oxygen isoelectronic

sequence using the methods developed by Badnell & Griffin (2001) thereby improving the accuracy of the collisional data still further.

Acknowledgements. The present calculations were carried out on the Cray T-90 and the Fujitsu VPP700 at the Leibniz-Rechenzentrum of the Bayerischen Akademie der Wissenschaften. The generous allocation of computer time and resources is gratefully acknowledged.

References

- Arnaud, M., & Rothenflug, R. 1985, *A&AS*, 60, 425
Badnell, N. R., & Griffin, D. C. 2001, *J. Phys. B*, 34, 681
Berrington, K. A., Eissner, W. B., & Norrington, P. H. 1995, *Comput. Phys. Commun.*, 92, 290
Bhatia, A. K., Fawcett, B. C., Lemen, J. R., et al., *MNRAS*, 240, 421
Bowyer, S., & Malina, R. F. 1991, in *Extreme Ultraviolet Astronomy*, ed. R. F. Malina, & S. Bowyer (Pergamon Press, New York), 397
Burgess, A., & Tully, J. A. 1992, *A&A*, 254, 436
Burke, V. M., & Seaton, M. J. 1986, *J. Phys. B*, 19, L527
Butler, K., & Zeippen, C. J. 2000, *A&AS*, 143, 483
Butler, K., & Zeippen, C. J. 2001, *A&A*, 372, 1078
Corliss, C., & Sugar, J. 1982, *J. Phys. Chem. Ref. Data*, 11, 135
Czaykowska, A., de Pontieu, B., Alexander, D., et al. 1999, *ApJ*, 521, L75
Eissner, W., Galavis, M. E., Mendoza, C., et al. 1999, *A&AS*, 136, 385
Eissner, W., Jones, M., & Nussbaumer, H. 1974, *Comput. Phys. Commun.*, 8, 270
Hummer, D. G., Berrington, K. A., Eissner, W., et al. 1993, *A&A*, 279, 298
Louergue, M., Mason, H. E., Nussbaumer, H., et al. 1985, *A&A*, 150, 246
Mewe, R., Gronenschild, E. H. B. M., & van den Oord, G. H. J. 1985, *A&AS*, 62, 197
Mewe, R., Lemen, J. R., & van den Oord, G. H. J. 1986, *A&A*, 65, 511
Nussbaumer, H., & Storey, P. J. 1978, *A&A*, 64, 139
Saraph, H. E. 1972, *Comput. Phys. Commun.*, 3, 256
Schrijver, C. J., Mewe, R., van den Oord, G. H. J., et al. 1995, *A&A*, 302, 438
Sugar, J., & Corliss, C. 1985, *J. Phys. Chem. Ref. Data*, 14, Suppl., 2, 498
Zhang, H. L., & Sampson, D. H. 2001, ADNDT, in preparation